Vacancy-solute interactions in Cu, Ni, Ag, and Pd

U. Klemradt, B. Drittler, T. Hoshino, R. Zeller, and P. H. Dederichs
Institut für Festkörperforschung, Forschungszentrum Jülich, D-5170 Jülich, Germany

N. Stefanou
Solid State Section, Department of Physics, University of Athens, GR-15771 Zografos, Athens, Greece
(Received 17 December 1990)

We apply the Korringa-Kohn-Rostoker Green's-function method and perform *ab initio* calculations based on local-density-functional theory for the vacancy-solute interaction energies in Cu, Ni, Ag, and Pd. In particular, we calculate the nearest-neighbor interaction of vacancies with 3*d* and 4*sp* impurities in Cu and Ni as well as with 4*d* and 5*sp* impurities in Ag and Pd. We also calculate the divacancy binding energies in these hosts. Further we demonstrate that the Hellmann-Feynman theorem with respect to the nuclear charge provides a useful tool to calculate and understand interaction energies. We discuss applications to jellium calculations for Cu and to the stability of larger agglomerates.

I. INTRODUCTION

The interaction of solute atoms with vacancies is of fundamental importance for the understanding of diffusion in dilute alloys, since a substitutional impurity can only migrate if a vacancy is present on a neighboring site. The first theoretical work on this problem is due to Lazarus,[1] who used Thomas-Fermi theory to describe the screening of the impurity. Despite the well-known deficiencies of this method the results[2] are more meaningful than one would expect. Deplanté and Blandin[3] extended this work by taking the oscillatory behavior of the screening into account. Using reasonable assumptions for the impurity phase shifts, they were able to obtain the correct trends for the interaction of 3*d* and 4*sp* impurities with vacancies in Cu, as our present calculations will demonstrate. Despite this very early and successful work, the further progress of the theory on this subject has been slow. Subsequent work has been based either on jellium models,[4] on pseudopotential-perturbation theory,[5,6] or on the tight-binding method.[7] Jellium models as well as pseudopotentials in connection with second-order perturbation theory can only be used for simple metals. Already impurities with nuclear charges $\Delta Z = \pm 1$ represent a problem for these methods,[6] and even more so do vacancies, as has been discussed by Evans.[8] For transition metals tight-binding calculations,[7] while containing a lot of physics, are notoriously plagued by unknown parameters. Thus, despite the numerous theoretical papers and the even larger amount of experimental work, the conclusion of Doyama[9] in 1978 still seems to be true: "Very few convincing experimental and theoretical values are available at present."

We have recently been able to perform realistic *ab initio* calculations for the vacancy-impurity interactions in Cu and Ni.[10] Calculations of vacancy formation energies have also been published.[11] The calculations are based on density-functional theory in the local-spin-density approximation and apply the Korringa-Kohn-Rostoker (KKR) Green's-function method for impurity calculations. While the potentials are assumed to be spherically symmetric atomic sphere potentials, the full anisotropy of the charge density is taken into account in evaluating the total energies. As an improvement of these results,[10] in the present paper cellular integrals are not approximated by integrals over atomic spheres but evaluated exactly using shape functions.[12] Details about the calculational procedure are described in Sec. II. The most important approximation of the present calculations is the neglect of lattice relaxations and of the resulting elastic interaction between the defects. In order to minimize these effects we only calculate the interaction of vacancies with impurities from the same row of the Periodic Table as the host. Thus, in Sec. III we present the central results of our paper, i.e., the interaction energies of vacancies with 3*d* and 4*sp* solutes in Cu and Ni hosts as well as with 4*d* and 5*sp* solutes in Ag and Pd hosts. We only calculate the dominating interaction on the nearest-neighbor sites and compare our results with the experimental information from diffusion and positron annihilation. In Sec. IV we present results for the interaction of divacancies in Cu, Ag, Ni, and Pd.

In Sec. V an alternative expression for the interaction energy is derived being based on the Hellmann-Feynman theorem as applied to the nuclear charge of the impurity. It allows a description of the interaction purely in electrostatic terms. Using this theorem we demonstrate in Sec. VI that jellium calculations for single impurities in Cu can indeed explain the qualitative trends for the vacancy-solute interactions in Cu, provided the calculations are performed accurately and consistently. As another application of the Hellmann-Feynman theorem, in Sec. VII we discuss the stability of larger agglomerates of impurities with small valence differences ΔZ using only the information available from the dimer interaction. In Sec. VIII we summarize the main results of the paper.

II. THEORETICAL METHOD

We employ density-functional theory in the local-density approximation of van Barth and Hedin[13] but with the parameters as determined by Moruzzi *et al.*[14] Our calculational method is based on multiple-scattering theory. The Green's function of the electrons which are multiply scattered by a collection of nonoverlapping muffin-tin potentials centered at positions $\mathbf{R}^n$, is expanded into eigensolutions of these spherically symmetric local potentials:[15]

$$G(\mathbf{r}+\mathbf{R}^n,\mathbf{r}'+\mathbf{R}^{n'};E) = \delta_{nn'}\sqrt{E}\sum_L Y_L(\hat{\mathbf{r}})R_l^n(r_<,E)H_l^n(r_>,E)Y_L(\hat{\mathbf{r}}') + \sum_{L,L'} Y_L(\hat{\mathbf{r}})R_l^n(r,E)G_{LL'}^{nn'}(E)R_{l'}^{n'}(r',E)Y_{L'}(\hat{\mathbf{r}}') , \quad (1)$$

in rydberg atomic units. The position vectors $\mathbf{r},\mathbf{r}'$ are restricted to the Wigner-Seitz cell and $r_<$ and $r_>$ are, respectively, the smaller and larger of $r=|\mathbf{r}|$ and $r'=|\mathbf{r}'|$. The subscript $L=(l,m)$ collectively denotes angular momentum quantum numbers and Y_L are real spherical harmonics. The irregular H_l^n and the regular R_l^n solutions of the radial Schrödinger equation for the nth muffin-tin potential at energy E are defined by their asymptotic behavior outside the muffin-tin sphere of radius $R_{\rm MT}$ ($r \geq R_{\rm MT}$):

$$H_l^n(r,E)=h_l(r\sqrt{E}) , \qquad R_l^n(r,E)=j_l(r\sqrt{E})+\sqrt{E}\,t_l^n(E)h_l(r\sqrt{E}) , \quad (2)$$

where j_l and h_l are the spherical Bessel and Hankel functions and t_l^n the usual t matrix for the nth single potential.

The information about the multiple scattering between muffin tins is contained in the structural Green's-function matrix $G_{LL'}^{nn'}$. It can be related to its counterpart for the host crystal by an algebraic Dyson equation:

$$G_{LL'}^{nn'}(E)= G_{LL'}^{0nn'}(E) + \sum_{n'',L''} G_{LL''}^{0nn''}(E)[t_{l''}^{n''}(E)-t_{l''}^{0n''}(E)]G_{L''L'}^{n''n'}(E) , \quad (3)$$

where the 0 superscript refers to the host. The equation describes correctly and in a very efficient way the embedding of the defect into the ideal crystal. In our calculation the angular momentum expansion in the Green's functions includes s, p, d, and f electrons.

Since we consider the interaction of two different impurities 1 and 2 on nearest-neighbor sites in a fcc lattice, we allow the potentials of these two atoms as well as the potentials of all nearest-neighbor host atoms to deviate from the host potentials. Therefore the n'' summation in Eq. (3) includes 20 atoms, the geometry of which is shown in Fig. 1. All nonequivalent atoms are numbered from 1 to 9. In solving the Dyson equation (3) we make use of the symmetry point group C_{2v} of the 20-atom cluster. The largest irreducible submatrix is then of size 92×92, instead of 320×320 for the unsymmetrized matrix.

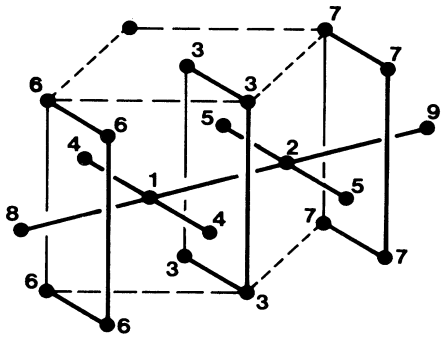

FIG. 1. Geometrical arrangement of two impurities (1 and 2) on nearest-neighbor sites in a fcc crystal. Also shown are all host atoms which are nearest neighbors to at least one of the impurities. The nonequivalent atoms are numbered from 1 to 9. The potential perturbations of all 20 atoms shown in the figure are calculated self-consistently.

The charge density is obtained from the Green's function by

$$n(\mathbf{r})=-\frac{2}{\pi}\int^{E_F} dE\ \mathrm{Im}G(\mathbf{r},\mathbf{r};E) . \quad (4)$$

For the valence states this integral is transformed into a contour integral in the complex energy plane[16] which can be calculated with rather few (64) energy points. The core electrons are allowed to relax.

For the calculation of the total energies we split the total energy in single-particle contributions $E_{\rm SP}$ and double-counting terms $E_{\rm DC}$. The single-particle contributions are given by[17]

$$E_{\rm SP}=\sum_i \varepsilon_i - E_F\left[\int n(\mathbf{r})d\mathbf{r}-N\right] \quad (5a)$$

$$=E_F N-\int^{E_F} d\varepsilon\, N(\varepsilon) , \quad (5b)$$

where N is the total number of electrons and $N(\varepsilon)$ the integrated density of states. The additional term $\sim E_F$ in (5a) guarantees that also non-particle-conserving charge densities $n(\mathbf{r})$ can be used without violating the extremal properties. The change of the integrated density of states $\Delta N(E)$ with respect to the host is evaluated by using a version of Lloyd's formula,[18] which is generalizable to complex energies:[17]

$$\Delta N(E)=\frac{2}{\pi}\sum_{n,L}\mathrm{Im}\ln\frac{\alpha_l^n(E)}{\alpha_l^{0n}(E)} - \frac{2}{\pi}\mathrm{Im}\ln\det|\delta_{nn'}\delta_{LL'}-G_{LL'}^{0nn'}(E)\Delta t_{l'}^{n'}(E)| . \quad (6)$$

The introduction of the $\alpha_l^n(E)$ functions, which are closely related to the phase shifts, ensures the correct analytical properties for complex energies, which is essential for the evaluation of $E_{\rm SP}$ by a contour integration.

The double-counting contributions E_{DC} can be written as[17]

$$E_{DC}=-\int d\mathbf{r}\, n(\mathbf{r})V_{\text{eff}}(\mathbf{r}) + \frac{1}{2}\left[\int d\mathbf{r}\, n(\mathbf{r})V_C(\mathbf{r})-\sum_n Z^n V_M(\mathbf{R}^n)\right] + \int d\mathbf{r}\, n(\mathbf{r})\varepsilon_{xc}(n(\mathbf{r}))\ . \quad (7)$$

Here $V_{\text{eff}}(\mathbf{r})$, the trial potential used in the Kohn-Sham equations, is a sum of spherically symmetric potentials. $V_C(\mathbf{r})$ and $V_M(\mathbf{r})$ are the Coulomb and the generalized Madelung potentials [see Eq. (12) below], which are evaluated with the full, i.e., nonspherically symmetric, charge densities.

For evaluating the potential energy E_{DC} we write all space integrals in (7) as sums of integrals over the Wigner-Seitz cells of the individual atoms. As it is natural for the multiple-scattering method we expand all relevant quantities, e.g., $n(\mathbf{r}), V_C(\mathbf{r}), \varepsilon_{xc}(\mathbf{r})$, in each cell n into spherical harmonics:

$$n^n(\mathbf{r})=\sum_L n_L^n(r)Y_L(\hat{\mathbf{r}}),\quad V_C^n(\mathbf{r})=\sum_L V_L^{cn}(r)Y_L(\hat{\mathbf{r}})\ . \quad (8)$$

The integrals over the Wigner-Seitz cells are then evaluated exactly by introducing a Heaviside unit-step function $\Theta(\mathbf{r})$, being equal to 1 within the Wigner-Seitz cell and zero otherwise, and by expanding $\Theta(\mathbf{r})$ into spherical harmonics:

$$\Theta(\mathbf{r})=\sum_L \Theta_L(r)Y_L(\hat{\mathbf{r}})\ . \quad (9)$$

The radial shape functions $\Theta_L(r)$, introduced by Andersen *et al.*,[19] can be calculated very accurately.[12] Since they scale with the lattice constant, they must be evaluated only once for each structure, e.g., fcc or bcc. They are continuous functions of r, but their derivative is discontinuous at certain r values, e.g., at the muffin-tin radius. The integrals over the Wigner-Seitz sphere of atom n then have the form

$$\int_{WS} d\mathbf{r} f^n(\mathbf{r})=\int d\mathbf{r}\Theta(\mathbf{r})f^n(\mathbf{r}) = \sum_{L'}^{l'_{\max}}\int_0^\infty dr\, r^2\Theta_{L'}(r)f_{L'}^n(r)\ . \quad (10)$$

Here $f^n(\mathbf{r})$ is a smooth function of $\mathbf{r}$, e.g., the product $n(\mathbf{r})V_C(\mathbf{r})$ occurring in the second term of Eq. (7). Due to the angular momentum cutoff of the Green's function at $l_{\max}=3$, the charge density $n^n(\mathbf{r})$ and the Coulomb potential $V_C^n(\mathbf{r})$ have only nonvanishing components n_L^n and V_L^{cn} up to $l=6$, so that the angular momentum expansion of the product $f(\mathbf{r})=n(\mathbf{r})V_C(\mathbf{r})$ has only nonvanishing components $f_{L'}^n$ up to $l'=12$. Therefore we find that an accurate evaluation of all cellular integrals occurring in (7) for the Coulomb and exchange-correlation energies is possible if in (10) we evaluate all terms up to $l'_{\max}=4l_{\max}$.

For spherical potentials entering into the Kohn-Sham equation we do not use muffin-tin potentials since they cannot describe the adjustment of the perturbed potentials in the interstitial region. Therefore, we prefer slightly overlapping potentials, which better fill up the volume. The simplest example is a spherically symmetric atomic sphere potential which has a sharp cutoff at the Wigner-Seitz radius. The calculations are actually performed using the $l=0$ component of the full cell potential $V_{\text{eff}}(\mathbf{r})$, which can be constructed from the full charge density. This potential has a smoother cutoff which is essentially determined by the shape function $\Theta_{l=0}(r)$. Test calculations show that for practical purposes both potentials give very much the same interaction energies.

In evaluating the integrals (10) and in solving the Kohn-Sham equations for central potentials truncated by $\Theta_{l=0}(r)$, the singularities of the Θ_L functions at certain critical radii require special care. Therefore we adjust our radial mesh to these radii and calculate the integral (10) piecewise from one critical radius to the next by Simpson's rule. Likewise we solve the radial Kohn-Sham equations separately in each interval using as initial conditions the value and slope at the last point of the previous interval.

III. VACANCY-SOLUTE INTERACTIONS

Figure 2 shows the calculated interaction energies of a vacancy with 4*d* and 5*sp* impurities in Ag and Pd. Positive energies mean a repulsion of the two defects, negative energies mean attraction. For the *sp* impurities in Ag and Pd one obtains an attraction roughly proportional to the valence difference ΔZ. Contrary to this, for the transition metal impurities the interaction is repulsive and shows a parabolic behavior with a maximum in the middle of the row. Note that the curve for the Pd host lies completely below the one for Ag, meaning that the repulsion of the 4*d* impurities is weaker in Pd than in Ag, whereas the attraction of the *sp* impurities is stronger.

4*d* impurities in Ag show a rather broad virtual bound state[15] being a result of the hybridization of the impurity 4*d* electrons with the 5*sp* electrons of Ag. The resulting 4*d*-5*sp* bonds are not as strong as the 4*d*-4*d* bonds of the elemental transition metal; therefore the solubility of 4*d* impurities in Ag is endothermic and rather small. Nevertheless this bonding is clearly stronger than the bonding

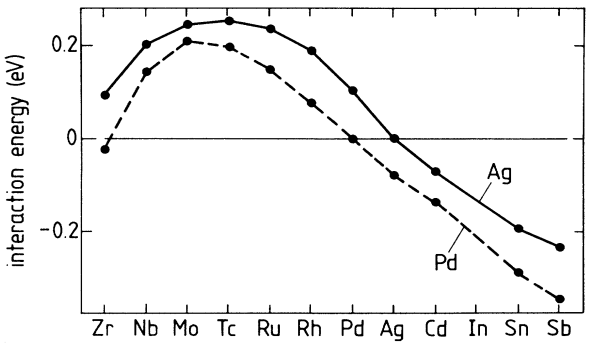

FIG. 2. Interaction energies of a vacancy with 4*d* and 5*sp* impurities in Ag and Pd. Positive energies mean repulsion; negative ones, attraction.

forces in pure Ag. Therefore by creating a vacancy it is more favorable to break such a Ag—Ag bond than the relatively strong 4*d*-5*sp* bond, meaning that the 4*d* impurity is repelled from the vacancy.

The parabolic behavior across the 4*d* series is a band-filling effect and is qualitatively very similar to the parabolic behavior of the cohesive energies as explained by Friedel. For the early 4*d* impurities only the lower "bonding" parts of the virtual bound state are occupied, whereas for the later 4*d* impurities also the higher antibonding states are filled. In the presence of a vacancy the virtual bound state of a nearby impurity becomes narrower due to the loss of hybridization which then explains the loss of bonding and the repulsion from the vacancy.

The calculated interaction energies for the 4*d* impurities look very much like a scaled-down version of the cohesive energies and the surface energies of the corresponding 4*d* metals. In these cases the much stronger 4*d*-4*d* host bond is responsible for the cohesion and has to be broken at the surface, which explains why these energies are so much larger. The parabolic behavior found in both cases is due to the same band-filling effect.

In Pd the interaction of 4*d* impurities with vacancies can be explained similarly. The interaction of the impurity 4*d* orbitals with the Pd 4*d* orbitals is stronger than the 4*d*-5*sp* bonds in Ag, but also the reference 4*d*-4*d* bonds of the Pd host are much stronger than the Ag—Ag bonds, so that in total the solute-vacancy repulsion is weaker than in Ag. This trend is expected to continue for a neighboring transition metal host like Rh, for which the curve of the interaction energies should fall totally below the one for Pd. In fact, for a host in the middle of the transition-metal series, say Tc, we expect that all impurities, whether 4*d* or 5*sp* ones, are attracted by the vacancy. The reason is very simple: Tc has the strongest cohesion in the 4*d* series, since all bonding states are occupied in the middle of the series. Therefore the 4*d*-4*d* bonds in Tc are stronger than the bonds with neighboring elements, so that the corresponding impurities should be attracted to the vacancy.

For the interactions of *sp* impurities with the vacancy we cannot offer any convincing, simple-minded picture in terms of bond strength and one-particle energies. Here the simplest possible explanation seems to be the electrostatic argument derived by the Hellmann-Feynman theorem in Sec. V. We therefore postpone this discussion until Secs. V and VI.

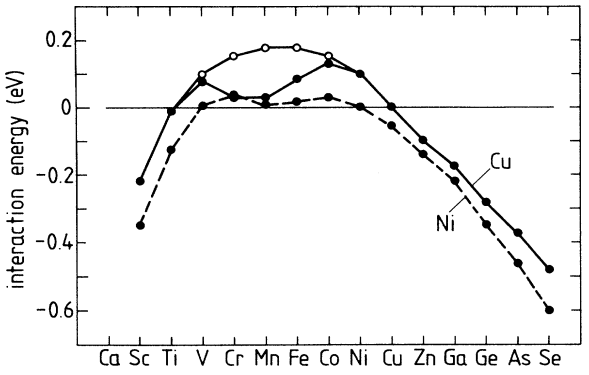

FIG. 3. Interaction energies of a vacancy with 3*d* and 4*sp* impurities in Cu (solid line) and Ni (dashed line). The open circles refer to non-spin-polarized calculations for 3*d* impurities in Cu.

Figure 3 shows the interaction energies of 3*d* and 4*sp* impurities with a vacancy both in Cu and Ni. Similarly to the results for Ag and Pd, the *sp* impurities are attracted by the vacancy, with the binding energy scaling with the valence difference ΔZ. However, the behavior of the 3*d* impurities in these hosts is very different from that of the 4*d*'s in Ag and Pd. This is due to the magnetic moments of the 3*d* impurities, which are absent in the 4*d* series. Indeed, calculations without spin polarization for Cu yield a similar parabolic dependence as found for 4*d* impurities in Ag (Fig. 2). The reduction of the interaction energies in the middle of the 3*d* series can then be explained as follows. On a neighboring site of the vacancy the hybridization of the 3*d* orbitals of the impurity with the host states is reduced. This leads to an enhancement of the local moments and to a corresponding gain of exchange energy. As a result one obtains, e.g., for Mn in Cu or Ni, only a small repulsive energy, since the loss of the bonding is counterbalanced by the gain of exchange energy.

A detailed comparison with experimental information about the solute-vacancy interaction is made in Table I for Cu, Table II for Ni, and Table III for Ag. Unfortunately, for Pd (Table IV) no experimental data are available. The most detailed information is available for

TABLE I. Solute-vacancy interaction energies calculated for 3*d* and 4*sp* impurities in Cu and compared with experimental data. The data marked by asterisks (δQ values) are the changes of the solute diffusion energies with respect to the self-diffusion energy of Cu and are taken from a recent data collection (Ref. 26). For their evaluation a self-diffusion energy for Cu of $Q_{\text{eff}}=2.14$ eV (Ref. 27) has been used. All values are given in eV.

	Sc	Ti	V	Cr	Mn	Fe	Co	Ni	Cu	Zn	Ga	Ge	As	Se
Theory	−0.22	−0.01	0.08	0.03	0.03	0.08	0.13	0.10	0	−0.10	−0.18	−0.28	−0.37	−0.48
Expt.	−1.30[a]	−0.11*	0.09*		−0.02*	0.09*	0.11*	0.19*	0	−0.07[b]	−0.10*	−0.23[c]	−0.31*	−0.27*
										−0.05[d]		−0.27[e]		
												−0.18[f]		

[a]Reference 45.
[b]Reference 23.
[c]Reference 20.
[d]Reference 24.
[e]Reference 21.
[f]Reference 22.

TABLE II. Same as Table I but for Ni host. The δQ values marked by asterisks have been evaluated from impurity diffusion data (Ref. 26) using a self-diffusion energy of $Q_{\text{eff}}=2.90$ eV for Ni (Ref. 28).

	Sc	Ti	V	Cr	Mn	Fe	Co	Ni	Cu	Zn	Ga	Ge	As	Se
Theory	−0.35	−0.13	0.01	0.04	0.01	0.02	0.03	0	−0.06	−0.14	−0.22	−0.35	−0.46	−0.60
Expt.								0	−0.27*			−0.20[a]	−0.30*	
												−0.50[b]		

[a]References 29–31.
[b]Reference 32.

Cu alloys. From positron-annihilation experiments in *Cu*Ge Triftshäuser and Jank[20] obtain a value of -0.23 ± 10 eV for the binding of the Ge impurity to the vacancy, whereas Doyama *et al.*[21] obtain a slightly larger value (-0.27 ± 10 eV). From vacancy-concentration measurements in *Cu*Ge Hehenkamp and Sander[22] deduce a binding energy of -0.18 ± 0.08 eV, which still compares reasonably well with our calculated value of -0.28 eV. From diffusion experiments in *Cu*Zn alloys Heumann[23] and Hagenschulte and Heumann[24] estimate binding energies of -0.07 and -0.05 eV, which are slightly smaller than our calculated value of -0.10 eV. Note that the binding energies obtained by diffusion and concentration measurement are high-temperature Gibbs free energies, which also contain some unknown entropic contribution. The extrapolation of these data to low temperature is difficult.[25] The other data in Table I, marked by an asterisk (δQ values), are obtained by solute diffusion measurements. They represent the difference between the impurity activation energy in Cu and the self-diffusion energy of Cu. While the determination of the binding energy from the diffusion data is a difficult process, one would nevertheless assume that the binding energy gives the most important contribution to the δQ values. For the 3*d* impurities, where only solute diffusion measurements are available, we find indeed a good correlation. Especially the small energy value for Mn, which is due to the large gain of magnetic exchange energy, as well as the binding energies for Sc and Ti, are well reflected in the diffusion measurements.

For the Ni host, only little experimental information is available. From positron-annihilation experiments Smedskjaer *et al.*[29] report a value of -0.20 ± 0.04 eV for the binding energy of a Ge impurity. The same value is also obtained by Faupel *et al.*[30] (-0.20 ± 0.06 eV) from solvent diffusion as well as by Mantl *et al.*[31] from tracer diffusion. From surface segregation in *Ni*Ge Lam *et al.*[32] estimate a value of -0.50 eV.

For the Ag-host, perturbed angular correlation measurements by Butt *et al.*[33] yield a binding energy of -0.19 ± 0.04 eV of an In impurity to the vacancy. Otherwise, only binding energies deduced from diffusion experiments[23–25,34–36] are available. For Cd, In, Sn, and Sb impurities these data correlate quite well with our calculations. (Note that we give no values for In in Ag and Pd. Because of numerical problems the host Green's functions for Pd and Ag are not reliable in the energy region of the 4*d* bound state of In. Therefore we cannot reliably calculate the binding energy of In. Its value can, however, be easily estimated from the neighboring elements Cd and Sn.) The reported δQ values for the 4*d* impurities Ru and Pd are positive, indicating a repulsion from the vacancy. While this is in qualitative agreement with our results, the cited values seem to be too large.

IV. DIVACANCY BINDING ENERGIES

Using the same method as for the impurity-vacancy interaction, we have calculated the binding energy E_{2V} of divacancies on nearest-neighbor sites in Cu, Ni, Ag, and Pd. The calculated binding energies are given in Table V; they all have about the same magnitude of about 0.07 eV. In a simple bond model one would expect that the divacancy binding energy is about $\frac{1}{6}$ of the vacancy formation

TABLE III. Solute-vacancy interaction energies calculated for 4*d* and 5*sp* impurities in Ag and compared with experimental data. The δQ values (Ref. 26) marked by asterisks have been evaluated using a self-diffusion energy of $Q_{\text{eff}}=1.97$ eV for Ag (Ref. 34) (all values in eV).

	Zr	Nb	Mo	Tc	Ru	Rh	Pd	Ag	Cd	In	Sn	Sb
Theory	0.09	0.20	0.24	0.25	0.23	0.19	0.10	0.0	−0.07		−0.20	−0.24
Expt.					0.88*		0.49*		−0.09[a]	−0.19[b]	−0.20[c]	−0.26[d]
									−0.07[a]	−0.18[e]	−0.18[f]	−0.20[e]
									−0.06[g]	−0.11[g]	−0.12[g]	−0.15[g]
									−0.04[g]	−0.09[g]		

[a]Reference 23.
[b]Reference 33.
[c]Reference 36.
[d]Reference 25.
[e]Reference 34.
[f]Reference 35.
[g]Reference 24.

TABLE IV. Same as Table III but for Pd host. No experimental values are available (all values in eV).

	Zr	Nb	Mo	Tc	Ru	Rh	Pd	Ag	Cd	In	Sn	Sb
Theory	−0.02	0.14	0.21	0.20	0.15	0.08	0	−0.08	−0.14		−0.30	−0.35

energy, since due to the agglomeration of two vacancies two bonds fewer are broken than for the isolated vacancies. The calculated values are however a factor of 2–3 smaller, indicating the importance of many-body forces. Note that our calculations do not include the effect of lattice relaxations. However, we do not expect this elastic interaction to be very important for the binding since the relaxation contribution to the formation energy of monovacancies is rather small, typically about 0.05 eV,[37] and since the relaxation contribution to the interaction should be only a fraction of this.

Experimental information about divacancy binding energies can be obtained from equilibrium measurements of vacancy concentrations. The results cited[38] for Au (0.32 eV) and Al (0.28 eV) are considerably larger than the values calculated here for Cu, Ni, Ag, and Pd. Note, however, that these data are obtained by fitting the non-Arrhenius behavior of the vacancy concentration by a two-vacancy model, which neglects any anharmonic temperature dependence of the formation energies. The cited values should therefore be considered with caution.

V. Z HELLMANN-FEYNMAN THEOREM FOR INTERACTION ENERGIES

Total energies are in general difficult to interpret especially since they are the differences of very large partial energies. This is a serious problem for the interaction energies because of their small values. Therefore it is desirable to have a formula for the interaction, which is to a large extent free from these disadvantages. Here we derive such an expression which is based on the Hellmann-Feynman theorem and which gives a direct relation of the interaction energies to the screening charge densities of the impurities. For the derivation we consider the nuclear charge Z_A of the defect A as an external continuous parameter.[39] The derivative dE/dZ_A of the total energy is given by

$$\frac{dE}{dZ_A}=\left.\frac{\partial E}{\partial Z_A}\right|_{n(\mathbf{r})}+\int d\mathbf{r}\frac{\delta E}{\delta n(\mathbf{r})}\frac{dn(\mathbf{r})}{dZ_A}$$
$$=V_M(\mathbf{R}_A)+E_F\ . \tag{11}$$

The first term, the derivative with respect to the explicit dependence of the functional $E\{n(\mathbf{r})\}$ on the nuclear charge Z_A, yields the generalized Madelung potential $V_M(\mathbf{r})$ at the nuclear position $\mathbf{R}_A$ due to all other nuclei and all electrons:

$$V_M(\mathbf{r})=\sum_{n\,(\neq A)}\frac{Z_n}{|\mathbf{r}-\mathbf{R}_n|}-\int d\mathbf{r}'\frac{n(\mathbf{r}')}{|\mathbf{r}-\mathbf{r}'|}\ . \tag{12}$$

The second term in (11) arising from the implicit dependence on Z_A yields the Fermi energy E_F because the considered states are always neutral and $\delta E/\delta n(\mathbf{r})=E_F$. The result (11) allows a simple classical interpretation: $V_M(\mathbf{R}_A)dZ_A$ is the energy gain obtained by increasing the nuclear charge against the Coulomb potential of all other charges, while $E_F dZ_A$ is the energy gain obtained by adding dZ_A electrons to the system in order to achieve neutrality. By integrating (11) from the host value Z_H to the true value Z_A of the impurity we obtain the energy difference $E(Z_A)-E(Z_H)$. In order to obtain a formula for the interaction energy ΔE between the defects A and B, we "create" the defect A once with defect B on a nearest-neighbor site and once without defect B, which is equivalent to defect B being infinitely far away. We obtain for the interaction energy

$$\Delta E=\int_{Z_H}^{Z_A}dZ'_A\{V_M(\mathbf{R}_A;Z'_A,Z_B)-V_M(\mathbf{R}_A;Z'_A,Z_H)\}\ , \tag{13}$$

where $V_M(\mathbf{R}_A;Z'_A,Z_B)$ is the Madelung potential at the nuclear site $\mathbf{R}_A$ of defect A with nuclear charge Z'_A, if the second defect has the charge Z_B.

In order to express (13) in terms of the charge density and the nuclear charges, we write $n(\mathbf{r})$ in the form

$$n(\mathbf{r})=n_0(\mathbf{r})+\Delta n_A(\mathbf{r})+\Delta n_B(\mathbf{r})+\Delta n_{AB}(\mathbf{r})\ . \tag{14}$$

Here $n_0(\mathbf{r})$ is the host density, $\Delta n_A(\mathbf{r})$ and $\Delta n_B(\mathbf{r})$ are the changes induced by the single defects Z_A and Z_B, whereas $\Delta n_{AB}(\mathbf{r})$ is the additional change due to the simultaneous presence of both defects. Then we obtain from (13)

$$\Delta E=\frac{\Delta Z_A\,\Delta Z_B}{|\mathbf{R}_A-\mathbf{R}_B|}-\Delta Z_A\int d\mathbf{r}\frac{\Delta n_B(\mathbf{r})}{|\mathbf{R}_A-\mathbf{r}|}$$
$$-\int_{Z_H}^{Z_A}dZ'_A\int d\mathbf{r}\frac{\Delta n_{AB}(\mathbf{r};Z'_A,Z_B)}{|\mathbf{R}_A-\mathbf{r}|}\ . \tag{15}$$

This is an exact relation for the interaction energy between defects A and B. The derivation by the Hellmann-Feynman theorem ensures that it is a difference of total energies and that it implicitly also contains the relevant kinetic and exchange-correlation energies. It clearly shows that ΔE is uniquely determined by the charge density, which however is needed for all intermediate charge states Z'_A. This is even true in the case of spin polarization where usually the total energy is ex-

TABLE V. Calculated binding energies E_{2V} of divacancies in different fcc metals (all values in eV).

	Cu	Ni	Ag	Pd
E_{2V}	0.076	0.067	0.079	0.11

pressed in terms of the charge density *and* the magnetization density. However, the advantages of the above formula must be paid for by the linear order, in which charge-density errors enter, as compared to second-order errors in the total-energy expression by virtue of its extremal properties. As we have shown in Ref. 10, in practical calculations reliable values for the interaction energies can be obtained from (13) if the Z'_A integral is evaluated with a step width of $\Delta Z = \frac{1}{2}$.

The main advantage of the Hellmann-Feynman expression is its simplicity, i.e., the direct relation to the potential and the charge density which enables an interpretation of the interaction in classical electrostatic terms. Clearly Eqs. (13) and (15) are not symmetrical in both nuclear charges Z_A and Z_B, as one would expect. Of course, a similar relation can also be obtained with intermediate nuclear charges Z'_B, if defect B is "created" in the presence of defect A. Also a symmetrical formula can be obtained, if both defects are "created" simultaneously.

For practical purposes the limiting case of a weak defect A with small ΔZ_A is most important. In this case the last term in Eq. (15) can be neglected, since it is proportional to $(\Delta Z_A)^2$. Then one obtains to first order in ΔZ_A

$$\Delta E \cong \Delta Z_A \, \Delta V_M^B(\mathbf{R}_A) = \Delta Z_A \left[\frac{\Delta Z_B}{|\mathbf{R}_A - \mathbf{R}_B|} - \int d\mathbf{r} \frac{\Delta n_B(\mathbf{r})}{|\mathbf{R}_A - \mathbf{r}|} \right], \qquad (16)$$

where $\Delta V_M^B(\mathbf{R}_A)$ is the change of the Madelung potential at site $\mathbf{R}_A$ with respect to the host value, if the defect B alone is present in the crystal. Note that no assumption is made about the strength of B. If in addition to A defect B is also weak, the interaction energy ΔE is proportional to $\Delta Z_A \, \Delta Z_B$, which is essentially the result of second-order pseudopotential theory.[5]

When we restrict ourselves to small valence differences ΔZ_A and consider the vacancy as the strongly disturbing defect B, so that $Z_B = 0$, then according to Eq. (16) the vacancy-induced change $\Delta V_M^0(\mathbf{R}_A)$ of the Madelung potential gives the slope of the ΔE curve at $Z_A = Z_H$. Due to the almost linear behavior of the ΔE curves for *sp* impurities (see Figs. 2 and 4), Eq. (16) should be a reliable approximation for these impurities. In Ref. 10 we have calculated in this way the distance dependence of the interaction energies for four shells around the vacancy. In all four hosts the nearest-neighbor interaction is the strongest. Especially for Cu and Ag the interaction for the further neighbors is much weaker and shows an oscillatory behavior.

It is clear that in an all-electron approach as the present one, the vacancy cannot be considered as a weak defect, since the valence difference $\Delta Z_A = -Z_A$ is extremely large. However just this assumption has been made in the historic work of Lazarus,[1,2] Deplanté and Blandin,[3] and others[4] which considered the noble metals as jellia with one valence electron and the vacancy as a weak defect with $\Delta Z_A = -1$. From our present knowledge about the electronic structure of the noble metals this is a doubtful procedure. In order to find out if such a very simple interpretation of the solute-vacancy interaction in the noble metals is possible, we have repeated these jellium calculations with the present state of the art, i.e., using density-functional theory. The main results are given in the next section and a more detailed account will be published elsewhere.[40]

VI. JELLIUM CALCULATIONS FOR Cu

In order to describe a substitutional impurity in jellium,[41] first we must remove the positive background charge density in a Wigner-Seitz sphere, thus creating a vacancy. In the center of the sphere we then put the nuclear charge of the considered impurity and let the electrons relax. In order to compare with the "host" charge density, we put the nuclear charge of Cu ($Z = 29$) in the center of the sphere, so that the Cu impurity in Cu jellium serves as the reference host system. Only the perturbed jellium charge density is recalculated and determined self-consistently. The calculations include angular momenta up to $l = 4$ and use an outer cutoff radius of 10 bohr radii for the range of the perturbing potential.

Figure 4 shows the change of the charge density due to

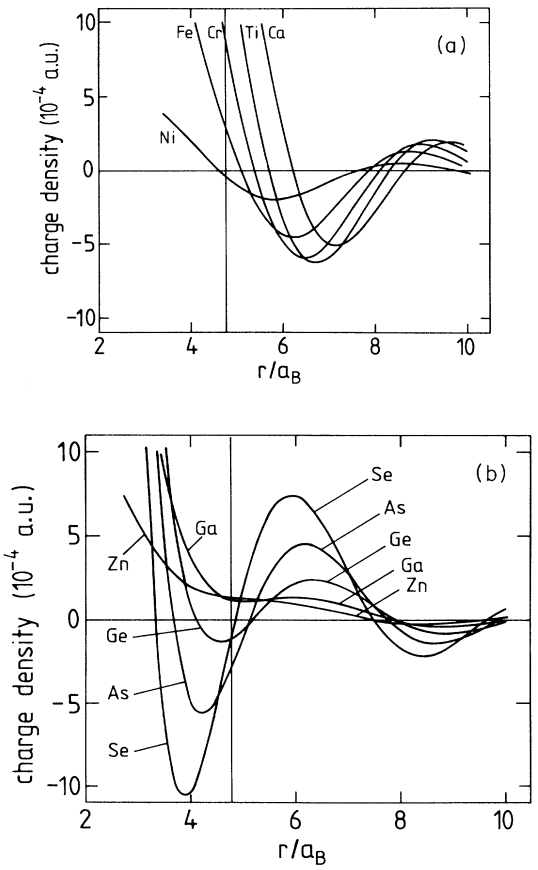

FIG. 4. Charge-density changes due to 3*d* impurities (a) and 4*sp* impurities (b) in a jellium corresponding to the valence density ($Z = 1$) of Cu. The vertical line indicates the nearest-neighbor distance R. The charge densities refer to calculations without spin polarization.

$3d$ impurities [Fig. 4(a)] and $4sp$ impurities in Cu [Fig. 4(b)]. For the *sp* impurities we observe for Zn and Ge a shallow minimum at the nearest-neighbor distance $R = 4.78 a_B$ which deepens and shifts inwards for the higher valent impurities. From these results it is clear that a Thomas-Fermi description[1,2] of the charge-density changes is completely wrong, since it yields a positive and exponentially decreasing charge density for the *sp* impurities. Thus, the approach of Lazarus[1] and Le Clair[2] for the interaction energies is unjustified and the good agreement obtained with the experiment is purely accidental. For the $3d$ impurities [Fig. 4(a)] we observe a positive charge-density change at the nearest-neighbor site which strongly increases with the valence difference.

In order to calculate the interaction energy in first-order perturbation theory [Eq. (16)], the change $\Delta V_M(r)$ of the Madelung potential induced by the impurities is needed. This is shown in Fig. 5 for $3d$ impurities (a) and $4sp$ impurities (b). For the transition-metal impurities only the results of paramagnetic calculations are given. In the sequence Ca to Ni the first maximum of the potential shifts strongly inwards, so that the potential at the nearest-neighbor site is always repulsive and strongest for Ti, when the maximum is at the nearest-neighbor distance R. For the $4sp$ impurities the potential is always attractive at R and roughly scales with the valence charge.

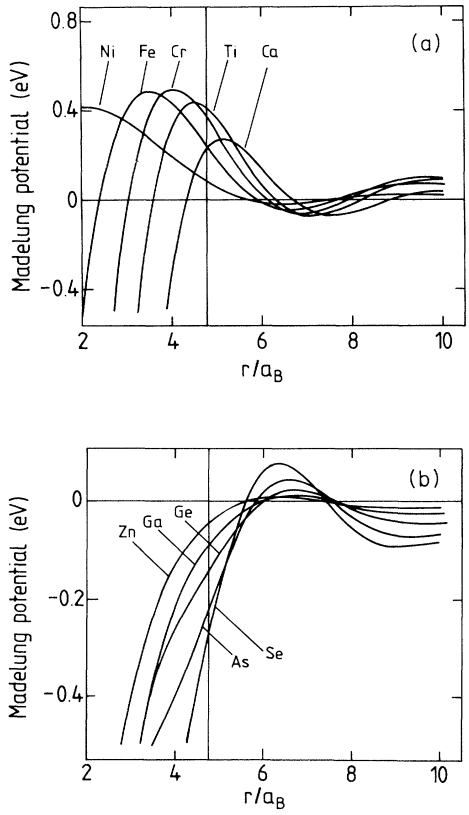

FIG. 5. Changes of the Madelung potential $\Delta V_M(r)$ due to $3d$ (a) and $4sp$ impurities (b) in Cu jellium. Spin polarization is not included in the calculation.

A more detailed discussion will be given elsewhere together with jellium results for Ag.[40]

For the interaction energy, according to Eq. (16) we need the perturbed Madelung potential at the nearest-neighbor distance, since the vacancy is considered as a substitutional defect with $\Delta Z = -1$. However this point-charge model for the vacancy is not consistent with the jellium approach, since in order to create a vacancy one must remove the positive background charge density in the whole Wigner-Seitz sphere of the vacancy. Therefore Eq. (16) has to be modified in such a way that the average of the potential $\Delta V_M(\mathbf{r})$ over the nearest-neighbor Wigner-Seitz sphere is taken. The averaging is done numerically. The effect of the averaging can also be studied analytically, if one expands the potential in a Taylor series around the nearest-neighbor distance R and averages each term separately. For symmetry reasons, the first-order term being proportional to the gradient of the potential vanishes. The second-order term containing the second derivaties of the potential can be evaluated using the Poisson equation relating $\Delta V_M(r)$ to the perturbed charge density $\Delta\rho(r)$. The third-order term again vanishes. Thus up to third order the average of the Madelung potential over the nearest-neighbor sphere is given by

$$\langle \Delta V_M(\mathbf{r}) \rangle \cong \Delta V_M(R) - \frac{2\pi}{5} R_{\mathrm{WS}}^2 \Delta\rho(R) , \tag{17}$$

where R_{WS} denotes the Wigner-Seitz radius. This equation describes the effect of the averaging qualitatively correct. Quantitatively it is, however, not reliable.

The results obtained for the interaction in the jellium model are shown in Fig. 6 together with the results obtained by the KKR Green's-function method. It is seen that both approaches give quite similar trends. The deviations essentially arise from the *d* band of Cu, which cannot be taken into account in the jellium model; a discussion of the origin of these differences will be given elsewhere.[40]

Averaging the potential over the nearest-neighbor

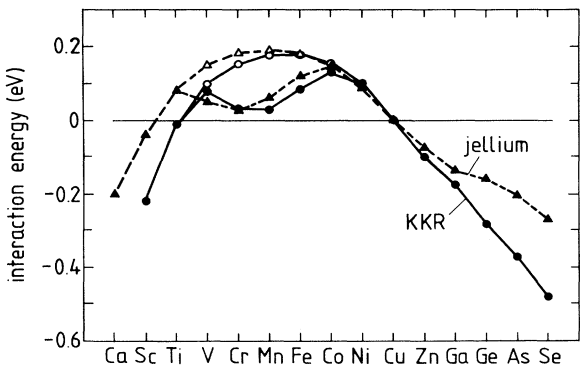

FIG. 6. Interaction energies of a vacancy with $3d$ and $4sp$ impurities in Cu as calculated in the jellium model (dashed line). Also shown are the total-energy results obtained by the KKR Green's-function method (see Fig. 3). Open symbols refer to calculations without spin polarization.

sphere is quite important, as comparison with $\Delta V_M(r)$ (see Fig. 5) shows. For instance, in the $3d$ series $\Delta V_M(R)$ has its maximum for Ti (0.43 eV) whereas the interaction energy ΔE is maximal for Mn (0.27 eV) and has a value of 0.16 eV for Ti. (These values refer to jellium calculations without spin polarization.) The difference is caused by the large charge perturbation $\Delta\rho(R)$ for the early-transition-metal impurities (see Fig. 4). Therefore the Madelung potential $\Delta V_M(r)$ deviates for smaller distances strongly from its value at R (see Fig. 5). On the contrary, for the sp impurities the corrections to the point-charge model are not very important, since the corresponding perturbed charge densities $\Delta\rho(R)$ are much smaller.

By summarizing we conclude that the jellium model together with the first-order perturbation theory gives a qualitatively correct description of the solute-vacancy interaction in Cu, both for the $3d$ as well as for the $4sp$ impurities. Therefore, it provides a very simple explanation of the interaction in terms of the Madelung potential of the single impurity. However, we have also shown that a consistent and reliable calculation of the Madelung potential is required. The close agreement found in earlier calculations[1-4] is more or less accidental and due to error cancellations of the different unreliable approximations involved. In the work of Deplanté and Blandin[3] these are, e.g., the use of the asymptotic formula for the Friedel oscillations, the rough estimate of the impurity phase shifts, and the point-charge model for the vacancy. Similar jellium arguments should also hold for the other noble-metal hosts, but of course, not for transition metals like Ni and Pd.

VII. LARGER AGGLOMERATES IN Cu AND Ag

As another interesting application of Eq. (16) we consider the agglomeration of a third impurity with small ΔZ_A to an already existing dimer complex which as a whole entity we identify now with defect B. Defect A might be an sp impurity like Zn or Ga for which we expect in analogy to the vacancy-solute energies (see Figs. 2 and 3) that the interaction energy with the dimer scales linearly with ΔZ_A, at least for small valence differences.

As a first example Fig. 7 shows the change of the Madelung potential $\Delta V_B^M(\mathbf{R}_A)$ for a divacancy in Ag. The heights of the column give the strength of the Madelung potential ΔV_B^M on the nearest-neighbor sites $\mathbf{R}^A$ of both vacancies which are numbered as in Fig. 1. Here and in the next figures downward columns mean negative values $\Delta V^M<0$ (e.g., binding of an impurity with $\Delta Z_A>0$), upward columns (dark) mean positive values. The potentials are only shown for sites 6, 3, and 7 from which the potentials on the other sites can be inferred. One finds that the binding on site 3, which are nearest neighbors to both vacancies, is about twice as strong as the binding on all other sites, being about equal for all sites which are nearest neighbors to only one of the vacancies. This is a consequence of two important facts. Firstly, the interaction with a single vacancy is strongly dominated by the nearest-neighbor interaction, as discussed in Ref. 10. Secondly, the interaction with both vacancies is in a good approximation additive, so that the binding energy on site 3 is about double the interaction energy for a single vacancy, whereas the interaction on the other sites is unperturbed by the second vacancy. Quite similar results are also found for the interaction with divacancies in Cu.

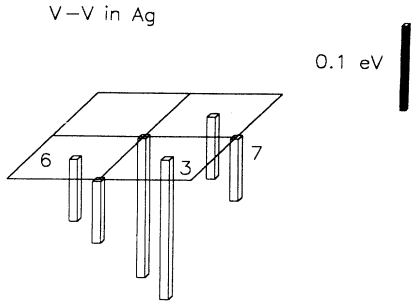

FIG. 7. Change of the Madelung potential induced on the nearest-neighbor sites 6, 3, and 7 (see Fig. 1 for explanation) by a divacancy V-V (on sites 1 and 2) in Ag. In first-order perturbation theory the interaction energy with an impurity is obtained by multiplication with ΔZ. For impurities with $\Delta Z>0$ downward columns mean attraction.

As a second example we consider the interaction of a Z_A impurity with a vacancy-solute dimer in Cu. Figure 8 shows the change of the Madelung potentials for dimers consisting of a vacancy on site 2 and a Ni, Zn, Ga, or Ge impurity on site 1. For an sp impurity with small $\Delta Z>0$ we find a weak attraction on sites 6, 4, and 8 which are adjacent to the Ni impurity only, a somewhat stronger attraction on the common neighboring sites 3, and a more or less unperturbed attraction to the vacancies on sites 7, 5, and 9. While the latter is also true for vacancy dimers with Zn, Ga, and Ge impurities, the behavior on the other sites changes drastically. On sites 6, 4, and 8 an sp impurity is strongly repelled, with the repulsion energy increasing almost linearly with the valence difference of the dimer impurity. On the common neighbor site 3 we have a balance between the attractive interaction with the vacancy and the repulsion with the impurity, so that for a Zn dimer these sites are still attractive but repulsive for the Ge dimer. In all cases we have studied, the interaction with the dimer can be well understood by superimposing the interaction of the Z_A impurity with the individual dimer defects and by restricting all interactions to nearest neighbors. A qualitatively similar behavior is also expected for the other hosts, i.e., Ag, Ni, and Pd. Clearly all these results are restricted to small ΔZ_A. The exact range of validity can only be found in more refined calculations. Nonperturbative results for the impurity-impurity interactions will be given elsewhere.[42]

Our calculations show that a single vacancy can bind more than one sp impurity, since the binding of the second impurity on positions 7, 5, and 9 is practically unchanged. The major change is a configurational one: of the 12 neighboring positions of the single vacancy five are blocked by the first impurity. By considering the ag-

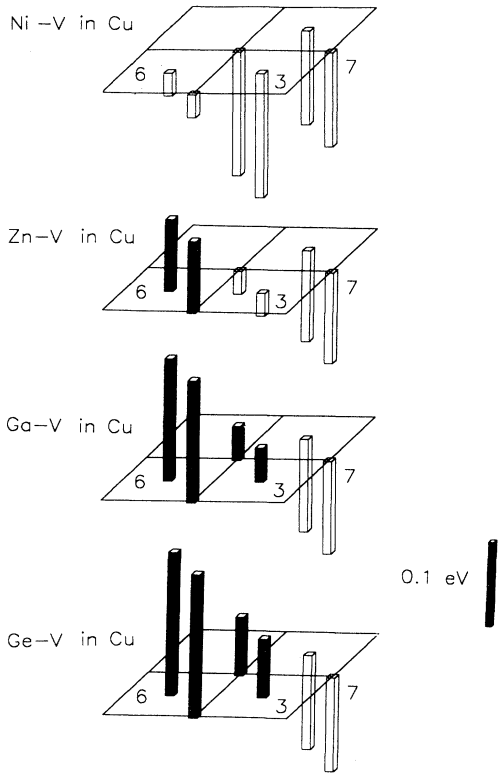

FIG. 8. Change of the Madelung potential induced on the nearest-neighbor sites 6, 3, and 7 by an impurity-vacancy X-V complex in Cu (impurities X = Ni, Zn, Ge on site 1; vacancy V on site 2; see Fig. 1 for explanation). The interaction energy with an additional impurity is obtained by multiplication with ΔZ. For $\Delta Z > 0$ upward columns (dark) mean repulsion, downward columns (open) mean attraction.

glomeration of further impurities in such a blocking picture, we find that at most four *sp* impurities can be bound to a single vacancy with the total binding energy roughly equal to four times the binding energy of a single impurity.

It is also experimentally well known that a vacancy in Cu can bind more than one *sp* impurity. This has been studied in detail in vacancy concentration measurements in *Cu*Ge alloys[22] and in solvent diffusion measurements in *Ga*Sn (Ref. 35) and *Ag*Sb (Ref. 43) alloys. Considerable binding of up to four *sp* impurities is found. The data are analyzed by the model of Dorn and Mitchel,[44] according to which the additional impurity occupies with equal probability one of the "free" nearest-neighbor positions of the vacancy. The binding energy for the additional impurities then slowly decreases with cluster size. Our above calculations suggest a different model, since two *sp* impurities strongly repel each other, e.g., in Cu two Ge impurities have a (repulsive) interaction of 0.39 eV.[42] Therefore, the number of sites available for the additional impurities is strongly reduced, i.e., for the third impurity only seven sites are available with roughly unperturbed binding, compared to 11 sites in the statistical model.[44] A reanalysis of the experimental data with our more realistic "blocking" model should lead to somewhat larger binding energies for the larger agglomerates.

VIII. SUMMARY AND CONCLUSION

The aim of this paper was to present accurate data for the interaction between vacancies and impurities in Cu, Ag, Ni, and Pd. We apply density-functional theory in the local-density approximation and solve the Kohn-Sham equations by using the KKR Green's-function method for impurity calculations. In order to minimize the effects of lattice relaxations which are not included in these calculations we consider only impurities from the same row of the Periodic Table as the host, i.e., 3*d* and 4*sp* impurities in Cu and Ni and 4*d* and 5*sp* impurities in Ag and Pd.

In all four hosts, *sp* impurities are strongly attracted to a nearest-neighbor site of the vacancy, with a binding energy roughly proportional to the valence difference ΔZ. In contrast to this, transition-metal impurities are repelled from the vacancies, with a maximal repulsion energy of about 0.2 eV in the middle of the 4*d* series. For 3*d* impurities in Ni and Cu magnetic exchange effects lower this repulsive energy considerably, so that a double hump structure of the interaction energy is observed. The calculated energies are in good agreement with the available experimental information.

By applying the Hellmann-Feynman theorem with the nuclear charge as a parameter we derive a new formula for the interaction energy which allows a simple electrostatic description of the interaction. Using this theorem we have shown that the trends for the vacancy-solute interaction in Cu can be easily understood within the jellium model, by considering the vacancy as a weak defect. As another application we discuss the stability of larger agglomerates, using only the information available from the dimer interaction.

ACKNOWLEDGMENTS

It is a pleasure to thank Th. Hehenkamp and H. Mehrer for helpful discussions concerning the experiments.

[1]D. Lazarus, Phys. Rev. **93**, 973 (1954).
[2]A. D. LeClaire, Philos. Mag. **7**, 141 (1962).
[3]J. L. Deplante and A. Blandin, J. Phys. Chem. Solids **26**, 381 (1965); A. Blandin, J. L. Deplante, and J. Friedel, J. Phys. Soc. Jpn. **18**, Suppl. II, 85 (1963).
[4]R. P. Gupta, Philos. Mag. B **41**, 169 (1980); Phys. Rev. B **22**, 5900 (1980).
[5]P. S. Ho and R. Benedek, IBM J. Res. Dev. **18**, 386 (1974); O. Takai, R. Yamamoto, M. Doyama, and S. Hisamatsu, Phys. Rev. B **10**, 3113 (1974).
[6]G. Solt and K. Werner, Phys. Rev. B **24**, 817 (1984).
[7]C. Demangeat, Ann. Phys. (Paris) **8**, 167 (1974); Acta Metall. **12**, 1521 (1974).
[8]R. Evans, in *Vacancies '76,* Proceedings of the Conference on

Point Defect Behaviour and Diffusional Processes, Bristol, 1976, edited by R. E. Smallman and F. E. Harris (The Metal Society, London, 1977), p. 30.
[9]M. Doyama, J. Nucl. Mater. **69&70**, 350 (1978).
[10]U. Klemradt, B. Drittler, R. Zeller, and P. H. Dederichs, Phys. Rev. Lett. **64**, 2803 (1990); U. Klemradt, Diploma thesis, Technical University Aachen, Aachen, Germany, 1989.
[11]B. Drittler, M. Weinert, R. Zeller, and P. H. Dederichs, Phys. Rev. B **42**, 9336 (1990).
[12]N. Stefanou, H. Akai, and R. Zeller, Comput. Phys. Commun. **60**, 231 (1990).
[13]U. von Barth and L. Hedin, J. Phys. C **5**, 1629 (1972).
[14]V. R. Moruzzi, J. F. Janak, and A. R. Williams, *Calculated Electronic Properties of Metals* (Pergamon, New York, 1978).
[15]P. J. Braspenning, R. Zeller, A. Lodder, and P. H. Dederichs, Phys. Rev. B **29**, 703 (1984).
[16]R. Zeller, J. Deutz, and P. H. Dederichs, Solid State Commun. **44**, 993 (1982); A. R. Williams, P. J. Feibelman, and N. D. Lang, Phys. Rev. B **26**, 5433 (1982).
[17]B. Drittler, M. Weinert, R. Zeller, and P. H. Dederichs, Phys. Rev. B **39**, 930 (1989).
[18]G. Lehmann, Phys. Status Solidi B **70**, 737 (1975).
[19]O. K. Andersen and R. G. Wooley, Mol. Phys. **26**, 905 (1973).
[20]W. Triftshäuser and R. Jank (unpublished).
[21]M. Doyama, K. Kuribayashi, S. Nanao, and S. Tanigawa, Appl. Phys. **4**, 153 (1974).
[22]Th. Hehenkamp and L. Sander, Z. Metallkd. **70**, 202 (1979).
[23]Th. Heumann, Z. Metallkd. **80**, 67 (1989).
[24]H. Hagenschulte and Th. Heumann, Phys. Status Solidi B **154**, 71 (1989).
[25]H. Hagenschulte and Th. Heumann, J. Phys. Condens. Matter **1**, 3601 (1989).
[26]*Diffusion in Solid State Metals and Alloys,* edited by H. Mehrer, Landolt-Börnstein, New Series, Group III, Vol. 26 (Springer-Verlag, Berlin, 1990).
[27]G. Rummel and H. Mehrer, Defect Diffusion Forum **66–69**, 453 (1989).
[28]K. Maier, H. Mehrer, E. Lessmann, and W. Schüle, Phys. Status Solidi B **78**, 689 (1976).
[29]L. C. Smedskjaer, M. J. Fluss, D. G. Legnini, M. K. Chason, and R. W. Siegel, *Proceedings of the Sixth International Conference on Positron Annihilation,* edited by P. G. Coleman *et al.* (North-Holland, Amsterdam, 1982).
[30]F. Faupel, C. Köstler, K. Bierbaum, and Th. Hehenkamp, J. Phys. F **18**, 205 (1988).
[31]S. Mantl, S. J. Rothman, L. J. Nowicki, and J. L. Lerner, J. Phys. F **13**, 1441 (1983).
[32]N. Q. Lam, P. R. Okamoto, and H. Wiedersich, J. Nucl. Mater. **74**, 101 (1978).
[33]R. Butt, R. Keitel, and G. Vogl, in Annual Report 1978 (Hahn-Meitner-Institut, Berlin, 1979), p. 68.
[34]S. J. Rothman, N. L. Peterson and J. T. Robinson, Phys. Status Solidi **39**, 635 (1970).
[35]Th. Hehenkamp and F. Faupel, Acta Metall. **31**, 691 (1983).
[36]F. Faupel and Th. Hehenkamp, Phys. Rev. B **34**, 2116 (1986).
[37]K. Abraham, Diploma thesis, Technical University Aachen, Aachen, Germany, 1990.
[38]R. W. Siegel, in *Properties of Atomic Defects in Metals,* edited by N. L. Peterson and R. W. Siegel (North-Holland, Amsterdam, 1978), p. 117.
[39]L. L. Foldy, Phys. Rev. **83**, 397 (1951).
[40]N. Stefanou (unpublished).
[41]J. Arponen, P. Hautojärvi, R. Nieminen, and E. Pajanne, J. Phys. F **3**, 2092 (1973); M. Manninen, P. Hautojärvi, and R. Nieminen, Solid State Commun. **23**, 795 (1977); R. M. Nieminen and M. J. Puska, J. Phys. F **10**, L123 (1980); M. J. Puska, R. M. Nieminen, and M. Manninen, Phys. Rev. B **24**, 3037 (1981); N. Stefanou, J. Phys. F **16**, 837 (1986).
[42]B. Drittler *et al.* (unpublished).
[43]Th. Hehenkamp, W. Schmidt, and V. Schlett, Acta Metall. **28**, 1715 (1980).
[44]J. E. Dorn and J. B. Mitchel, Acta Metall. **14**, 17 (1966).
[45]A. S. Berger and R. W. Siegel, J. Phys. F **9**, L67 (1979).